

1 **Foliar Sieve Elements: Nexus of the Leaf**

2

3 William W. Adams III^{a,*}, Jared J. Stewart^a, Stephanie K. Polutchnko^a, Barbara Demmig-Adams^a

4

5 ^a Department of Ecology and Evolutionary Biology, University of Colorado, Boulder, Colorado,
6 USA; william.adams@colorado.edu; jared.stewart@colorado.edu;
7 stephanie.polutchnko@colorado.edu; barbara.demmig-adams@colorado.edu

8

9 *Corresponding author. Email: william.adams@colorado.edu, phone: +1-303-492-2880

10

11 **Highlights**

12 • Foliar sieve element features varied with growth environment and among species

13 • Foliar sieve element features covaried with features of multiple leaf systems

14 • Foliar sieve element volume correlated with photosynthetic capacity

15 • Foliar sieve element features correlated with leaf thickness

16 • Features of sieve elements correlated with those of other vascular cells

17

18 **Abstract**

19 In this review, a central position of foliar sieve elements in linking leaf structure and function is
20 explored. Results from studies involving plants grown under, and acclimated to, different
21 growth regimes are used to identify significant, linear relationships between features of minor
22 vein sieve elements and those of 1) leaf photosynthetic capacity that drives sugar synthesis, 2)
23 overall leaf structure that serves as the platform for sugar production, 3) phloem components that
24 facilitate the loading of sugars (companion & phloem parenchyma cells), and 4) the tracheary
25 elements that import water to support photosynthesis (and stomatal opening) as well as mass

26 flow of sugars out of the leaf. Despite comprising only a small fraction of physical space within
27 the leaf, sieve elements represent a hub through which multiple functions of the leaf intersect. As
28 the conduits for export of energy-rich carbohydrates, essential mineral nutrients, and information
29 carriers, sieve elements play a central role in fueling and orchestrating development and function
30 of the plant as well as, by extension, of natural and human communities that depend on plants as
31 producers and partners in the global carbon cycle.

32

33 Keywords: foliar vasculature, minor veins, phloem, photosynthesis, sieve elements, tracheary
34 elements

35

36 Abbreviations: Companion cell (CC), phloem parenchyma cell (PC), vein density (VD)

37

38 **1. Introduction**

39 Compared to other leaf cells, sieve elements are diminutive with a small cross-sectional area
40 when viewed perpendicularly to the long axis of a vein (Esau 1977; Adams et al., 2013; Cohu et
41 al., 2013a, 2014; Muller et al., 2014a,b; Stewart et al., 2017a). Sieve elements also comprise the
42 smallest single tissue fraction of foliar veins (Cohu et al., 2013a, 2014; Muller et al., 2014a,b;
43 Stewart et al., 2016, 2019) or the leaf as a whole (Esau, 1977; Muller et al., 2014b).

44 Nevertheless, the sieve element plays an outsize role in the leaf. During leaf emergence and
45 initial expansion, sieve elements of the newly formed primary and secondary, or major, veins are
46 conduits for the import of sugars that provide the fuel and structural building material for leaf
47 construction (Turgeon and Webb, 1973; Schmalstig and Geiger, 1987; Gagnon and Beebe,
48 1996). As the leaf expands, chloroplasts in foliar mesophyll cells become photosynthetically

49 competent, stomata become functional, and sugar produced in the leaf exceeds the needs of the
50 leaf. At this point, the leaf undergoes transition from a sink for sugar (wherein consumption
51 exceeds production) to a source of sugar (wherein production exceeds consumption) and,
52 consequently, flow in the sieve elements reverses (Fellows and Geiger, 1974; Turgeon, 1989). In
53 some species, this physiological shift coincides with the maturation of an intricate network of
54 higher-order, or minor, veins that develops from the major veins into the mesophyll tissue during
55 expansion (Turgeon, 2006). Collectively, the cells in these minor veins (as well as major veins
56 in some species; see Turgeon, 2006) support active and regulated processes by which sugars are
57 moved from the sugar-producing mesophyll cells into the sugar-transporting phloem network
58 (Rennie and Turgeon, 2009; Zhang and Turgeon, 2018). The sieve elements within these minor
59 veins are the primary focus of this review. In many instances, we refer specifically to the
60 vascular cells of minor veins in herbaceous annual eudicots, such as sunflower (Fig. 1A; Stewart
61 et al., 2019; see also Wang and Canny, 1985) and *Arabidopsis thaliana* (Fig. 1B; Stewart et al.,
62 2019; see also Haritatos et al., 2000). In other cases, in which minor veins are not invoked, the
63 statements and discussion involve all the foliar vasculature (every order of vein from midrib to
64 the smallest veinlet).

65

66 **2. Relationship to Photosynthesis**

67 One may expect coordination between photosynthetic activity and leaf components that interact
68 with photosynthesis. Coordination between stomatal opening and photosynthesis maximizes
69 production of photosynthate while limiting water loss (Lawson et al., 2018). Regarding foliar
70 vascular tissues, numerous studies have documented the important role of the water distribution
71 network (via the xylem) that supports the leaf and photosynthesis (for reviews, see Adams et al.,

72 2018a; Brodribb and Buckley, 2018). In addition to coordination of water flux and
73 photosynthetic activity, the anatomical and ultrastructural infrastructure of the vasculature
74 exhibits acclimatory adjustments in concert with adjustments in maximal photosynthetic capacity
75 (Adams et al., 2013, 2016, 2018a; Cohu et al., 2013b; Stewart et al., 2016, 2017a,b). Whereas
76 relationships were reported between photosynthetic capacity and minor vein tracheary element
77 features, these were less significant than relationships between transpiration rate and water-
78 transport infrastructure (Cohu et al., 2013b; Adams et al., 2016, 2018a, 2018b). On the other
79 hand, relationships between photosynthetic capacity and sieve element numbers and/or volumes
80 were typically highly significant (Cohu et al., 2013b; Muller et al., 2014a; Adams et al., 2016,
81 2018a; Stewart et al., 2019). In other words, acclimatory changes in the capacity for
82 photosynthesis were typically most aligned with changes in sieve-element infrastructural
83 capacity.

84 To illustrate some of these relationships, Fig. 2 shows data from several studies of a
85 summer and a winter annual after acclimation to various growth light and temperature regimes.
86 For this comparison with photosynthesis expressed per unit leaf area, sieve element features are
87 scaled to the leaf level either (Fig. 2A) as the product of sieve element number per minor vein \times
88 length of vein per leaf area (vein density) or (Fig. 2B) as the product of sieve element cross-
89 sectional area per minor vein \times length of vein per leaf area, which approximates sieve element
90 volume per leaf area (Stewart et al., 2019). It had previously been shown that the number of
91 sieve elements per foliar minor vein, which is greater in winter annuals grown under high versus
92 low light intensities or grown under low versus high temperatures, can show significant, linear
93 relationships with photosynthetic capacity when vein density varies very little (Cohu et al.,
94 2013b). For comparisons of species with varying vein density, highly significant relationships

95 were obtained for sieve element features scaled to the leaf level by multiplication of vein density
96 (Muller et al., 2014a; see also Stewart et al., 2019), as done here (Fig. 2A) for sunflower and *A.*
97 *thaliana*. The trait of a higher vein density in sunflower leaves compared to leaves of *A. thaliana*
98 (Cohu et al., 2014) is likely important for a summer annual that experiences a greater rate of
99 transpirational water loss per unit leaf area during its growing season compared to a winter
100 annual. Similarly, species growing in more arid environments possessed greater foliar vein
101 density compared to species from more mesic habitats (Dunbar-Co et al., 2009; de Boer et al.,
102 2016), presumably resulting in enhanced distribution of water throughout the leaf (de Boer et al.,
103 2016).

104 The volume of minor-vein sieve elements per unit leaf area can likely serve as a proxy for
105 the flux capacity for photosynthate export. It is noteworthy that sieve-element volume exhibited
106 a single highly significant positive linear relationship with photosynthetic capacity with
107 overlapping data for sunflower and *A. thaliana* (Fig. 2B), whereas the sieve-element number
108 scaled to the leaf level exhibited two distinct relationships (each significant) with photosynthetic
109 capacity for the two species (Fig. 2A). This divergence between species was associated with a
110 greater number of sieve elements in the minor veins of *A. thaliana* than those of sunflower (Cohu
111 et al., 2013a, 2014; Muller et al., 2014a; Fig. 1). One can conclude that the greater vein density
112 of sunflower did not compensate for the lower number of sieve elements per individual vein,
113 thereby causing sunflower to have lower numbers of sieve elements at the leaf scale. Each
114 individual sieve element is thus also larger in sunflower compared to *A. thaliana* (Fig. 1), which
115 contributes to the single relationship with photosynthetic capacity for sieve element volume per
116 leaf area (Fig. 2B).

117 For a relationship between photosynthetic capacity and the features of tracheary
118 elements, the situation was reversed in the following way. There was considerable overlap of the
119 data resulting in a single significant positive relationship between the number of tracheary
120 elements scaled to the leaf level (number per minor vein \times vein density) and photosynthetic
121 capacity for the two species (Fig. 2C). On the other hand, there were two separate (but each
122 significant) positive relationships for the two species between tracheary element volume per leaf
123 area and photosynthetic capacity (Fig. 2D). This scenario indicates that (i) a lower number of
124 tracheary elements per vein (Fig. 1) and a greater vein density in sunflower compared to *A.*
125 *thaliana* resulted in the same number of tracheary elements per leaf area and (ii) individual
126 tracheary elements must also be larger in sunflower than in *A. thaliana* (Fig. 1; see also Cohu et
127 al., 2014). To summarize, sieve elements were less numerous at the leaf scale but of larger
128 individual size, while tracheary elements were both similarly numerous (at the leaf scale) and of
129 larger individual size in the summer annual sunflower compared to the winter annual *A. thaliana*.
130 This difference suggests a disproportionately greater emphasis on water transport in summer
131 annuals versus winter annuals by virtue of a combination of tracheary element number at the
132 scale of the individual vein, individual size of these water conduits, and vein density (cf. Cohu et
133 al., 2014).

134

135 **3. Relationship to Leaf Thickness**

136 We previously documented a significant linear relationship between the thickness of the layers of
137 the leaf's palisade cells and (i) sieve element cross-sectional area per veins as well as (ii) sieve
138 element number at the leaf scale (number per minor vein \times vein density) for two summer and
139 two winter annuals (Cohu et al., 2014). These relationships are similarly significant for the

140 thickness of the entire leaf shown here for sunflower and the winter annuals *A. thaliana* and
141 spinach (Fig. 3), indicating considerable coordination between overall leaf morphology and the
142 conduits for photosynthate export. It is noteworthy that the data points for the summer annual
143 clustered at a lower maximal leaf thickness as well as a lower maximal sieve element number at
144 the leaf scale and a lower maximal sieve element volume per leaf area. Furthermore, the two
145 winter annuals also varied in maximal leaf thickness and sieve element features at the leaf scale.
146 We previously showed that winter annuals, but not summer annuals, increase the number of
147 palisade layers when grown under cool temperature and high light compared to warm
148 temperature and moderate light (Cohu et al., 2014). The particularly thick leaves of spinach
149 could possibly also be associated with this species' membership in the Chenopodioideae
150 (subfamily of Amaranthaceae) that includes many halophytes with succulent properties
151 (Piirainen et al., 2017). In any event, it is noteworthy that sieve-element infrastructure closely
152 mirrored these differences in leaf thickness.

153

154 **4. Relationship Among Minor Vein Vascular Cell Types**

155 Adjustments in sieve-element infrastructure features also closely mirror those of the other
156 vascular cell types (Fig. 4). At the scale of the individual minor vein, there were significant
157 linear relationships between cross-sectional area of sieve elements per minor vein and either (i)
158 cross-sectional area of all other phloem tissue per minor vein (companion and parenchyma cells;
159 Fig. 4A) or (ii) cross-sectional area of tracheary elements per minor vein (Fig. 4B). The
160 correlation coefficients for both relationships further increased when all three metrics were
161 scaled to the leaf level (Fig. 5) by multiplying cross-sectional areas per minor vein \times vein
162 density, which results in volumes per leaf area (Stewart et al., 2019). While matching trends

163 among adjustments in the various vascular cell types may partly be due to developmental
164 constraints, it should be noted that there are also functional ties. All minor-vein vascular tissues
165 make contributions to sugar loading and export through the sieve elements. The phloem
166 parenchyma and companion cells both facilitate the flux of sucrose and active loading (in those
167 species that employ active loading) into the sieve elements (Ayre and Turgeon, 2018). Likewise,
168 in addition to supplying water to the leaf in support of stomatal opening, the tracheary elements
169 supply water to the sieve elements in support of mass flow of sugars out of the leaf for
170 distribution to the rest of the plant (Carvalho et al., 2018; Hesse et al., 2019). This theme is
171 further considered in the following section.

172

173 **5. Sieve Elements Transport More Than Sugars**

174 Most of the water that passes through the foliar tracheary elements of C₃ and C₄ plants is lost to
175 the atmosphere through transpiration, an inevitable consequence of stomatal opening that is
176 required for adequate diffusion of carbon dioxide into the leaf to support photosynthetic
177 production of sugars. This loss of water also contributes to cooling of leaves and prevention of
178 heat damage under high ambient temperatures and when there is a steep water potential gradient
179 between leaf and atmosphere. Only a negligible fraction of the water that enters a leaf is
180 consumed in metabolism (such as water splitting for photosynthesis, catabolic hydrolysis of
181 molecules, etc.). The major fraction of the remaining water fluxes from tracheary elements to
182 phloem and ultimately into sieve elements as it follows a water potential gradient fueled by the
183 concentration of solutes (sugars) in these sugar conduits (Hölttä et al., 2006; Nikinmaa et al.,
184 2013). Although these fates are mutually exclusive, their consequences are inherently linked
185 since stomatal opening is required for the production of sugars in quantities suitable for export

186 and the export of sugars from leaves is required for continued growth and maintenance of water-
187 acquiring roots. Moreover, sugar export from leaves, expression of associated genes, and
188 allocation to roots can be enhanced under water-limited conditions (e.g., Durand et al., 2016),
189 which suggests the fraction of water allocated to the sieve elements works synergistically, rather
190 than competitively, with the fraction allocated to support stomatal opening. However, to our
191 knowledge, the proportion of water transferred to the phloem versus that lost to the atmosphere
192 has not been quantified, but it is likely that several factors related to plant genotype (evolutionary
193 history), developmental stage, environmental conditions (e.g., water and nutrient availability)
194 during plant development, and prevailing environmental conditions at any given time contribute
195 to determining the relative fate of water delivered to the leaf via the xylem.

196 The function of sieve elements is consistent with the significant positive relationship
197 between cross-sectional areas per vein (Fig. 4B) and volumes per leaf area (Fig. 5B) of tracheary
198 elements and sieve elements. Sugars and associated water influx into sieve elements create
199 positive pressure at the source that, coupled with sugar unloading and water efflux in distant sink
200 tissues (and the resultant lowering of pressure within the phloem), drives mass flow of the sugar-
201 laden sap. This water-circulatory system between xylem and phloem continuously cycles water
202 back and forth between roots and shoots (van Bel, 2003; Hölttä et al., 2006), driven by newly
203 produced photosynthate during the day and sugars remobilized from stored starch at night
204 (Fondy and Geiger, 1982; Schleucher et al., 1998; Weise et al., 2003). Foliar sieve elements are
205 thus active in sugar export 24 h a day, thereby keeping the rest of the plant supplied with energy
206 and building material, regardless of photoperiod length (Mengin et al., 2017; Sharkey, 2017).

207 Since the primary function of the mature leaf is to produce and export energy-rich
208 carbohydrate, coordination should be expected between photosynthetic activity and the phloem

209 cells that participate in sugar export from the leaf. In addition to sieve elements, these include
210 cells that facilitate loading of photosynthate (all three species examined here are apoplastic
211 loaders) via sucrose efflux channels (SWEET proteins; Chen et al., 2012; Eom et al., 2015; Ayre
212 and Turgeon, 2018), ATPases (that pump protons into the apoplastic space; Offler et al., 2003;
213 Sondergaard et al., 2004; Gaxiola et al., 2007; Falhof et al., 2016; Ayre and Turgeon, 2018), and
214 sucrose-proton symporters (that move sucrose into the companion cells and, in some species, the
215 sieve elements; Srivastava et al., 2008; Rennie and Turgeon, 2009; Slewinski et al., 2013; Duan
216 et al., 2014; Ayre and Turgeon, 2018). The data presented here demonstrate coordination
217 between adjustments in the anatomical bases of photosynthesis and of sugar export during leaf
218 development. Up- and downregulation of photosynthetic function, i.e., light- and CO₂-saturated
219 maximal rate of photosynthesis per leaf area is associated with up- and down-sizing of leaf
220 infrastructure for photosynthesis as can be assessed, e.g., as leaf thickness (Demmig-Adams et
221 al., 2017). It may be possible to incorporate more photosynthetic protein into a single existing
222 chloroplast and more chloroplasts into an existing palisade cell (that could expand in length;
223 Amiard et al., 2005). However, major adjustments in photosynthetic capacity are often
224 associated with infrastructural change during leaf development, such as insertion of additional
225 palisade cell layers (Amiard et al., 2005; Dumlaor et al., 2012; Cohu et al., 2014; Adams et al.,
226 2016, 2018a).

227 A similar principle is apparently at work with respect to leaf vascular infrastructure. It is
228 unclear to what extent existing phloem cells involved in sugar loading may be able to insert
229 additional SWEET proteins, ATPases, or sucrose-proton symporters. However, the data shown
230 here clearly indicate that more and/or larger cells are formed during the development of leaves
231 that feature a greater photosynthetic capacity. This infrastructure expansion may increase the

232 membrane area available for placement of proteins that facilitate phloem loading as well as
233 plasmodesmatal passages for sugar flux (see discussion in Adams et al., 2013, 2016, 2018a,b;
234 Cohu et al., 2013b). The greater leaf-level volume of sugar-export conduits (sieve elements),
235 and water conduits (tracheary elements) during acclimation to different growth environments
236 presumably favors greater flux volumes. The selective pressure underlying the lowering of
237 photosynthetic capacity (and number of photosynthetic proteins) in growth environments that
238 permit, or require, less photosynthetic activity is understood to be the considerable cost of
239 protein synthesis and turnover (Ishihara et al 2017). The selective pressures that resulted in the
240 accompanying downsizing of sugar- and water-transport infrastructure are less well understood.
241 What is clear is that there is tight coordination in the anatomy of multiple leaf components across
242 species and environments (Adams et al., 2016, 2018a). For the case of photosynthesis,
243 coordination of functional and anatomical aspects is orchestrated via transcriptional control by
244 high-hierarchy gene regulators that respond to environmental cues and, in turn, control hundreds
245 of other regulators (see, e.g., Demmig-Adams et al., 2018). A key example for the transduction
246 of environmental cues are redox-modulated transcription factors (Hüner et al., 2016). Change in
247 the growth environment typically leads to the generation of redox signals in the chloroplast
248 (Demmig-Adams et al., 2014a,b, 2018) that are also relayed to the transcriptional control of
249 nuclear genes (via redox-based chloroplast-nucleus retrograde signaling; Leister, 2019; Unal et
250 al., 2020). It is likely that these same controls also coordinate function and anatomical features
251 of sugar- and water-transport systems with those involved in the photosynthetic production of
252 sugars.

253 In addition to photosynthate and water, a range of other molecules utilize the sieve
254 elements to move from the leaves to other parts of the plant (van Bel, 2003). Many essential

255 elements are remobilized from leaves to growing sinks. These mobilized substances include
256 various molecules containing nitrogen (e.g., amino acids, urea, nitrate; van Bel, 1990; Gaufichon
257 et al., 2013; Bohner et al., 2015; Tegeder and Hammes, 2018; Tegeder and Masclaux-Daubresse,
258 2018; Babst et al., 2019; Ninan et al., 2019; Sample and Babst, 2019), phosphate, sulfate, and
259 potassium (Khan and Choudhuri, 1992; Ning et al., 2013; Jeong et al., 2017), and the mineral
260 micronutrients iron, zinc, copper, sodium, and chloride (Jeschke and Pate, 1995; Römhild and
261 Schaaf, 2004; Shi et al., 2012; Barunawati et al., 2013; Pearce et al., 2014), although the
262 mobilization of the latter seen in herbaceous plants does not appear to occur in evergreen trees
263 during autumn (Shi et al., 2011).

264 In addition to transporting energy carriers, nutrients, and building blocks, sieve elements
265 transport information carriers used for long-distance signaling (for a recent, comprehensive
266 review, see Koenig and Hoffmann-Benning, 2020). These include at least five classes of
267 phytohormones, multiple lipids, many proteins, and messenger RNAs (some coding for proteins
268 transported in the phloem). These information carriers orchestrate a coordinated response of all
269 plant organs during development and/or in response to changes in environmental conditions
270 (Koenig and Hoffmann-Benning, 2020). Redox signals generated in chloroplasts and
271 mitochondria (Demmig-Adams et al., 2014a,b, 2018) tie developmental and environmentally-
272 induced changes in the leaf's energy metabolism to long-distance signaling by way of, for
273 example, redox modulation of the synthesis, sequestration, and transport of various
274 phytohormones (Foyer and Noctor, 2009; Demmig-Adams et al., 2013; Hüner et al., 2016;
275 Schippers et al., 2016; Srivastava et al., 2017; Tognetti et al., 2017).

276 Some of these signals originate in the sieve elements of the leaves. For instance, plastids
277 of sieve elements (and those of companion cells) are sites of jasmonic acid synthesis (Hause et

278 al., 2003), and both jasmonic acid and its precursor 12-oxo-phytodienoic acid (OPDA) are
279 exported from the leaf via the sieve elements (Koenig and Hoffmann-Benning, 2020). Jasmonic
280 acid signaling is an example of how environmental cues from biotic and abiotic stressors (Ali
281 and Baek, 2020; Pérez-Alonso et al., 2021) are transduced to an internal response, such as
282 formation of reactive oxygen species that oxidizes fatty acids of membrane phospholipids to
283 derivates such as OPDA and jasmonic acid (Demmig-Adams et al., 2017), which act as gene
284 regulators. Both OPDA and jasmonic acid can trigger wall/membrane invagination of phloem
285 transfer cells in leaf minor veins (Amiard et al., 2007). In turn, the level of such invaginations
286 was correlated with photosynthetic capacity in several species (Adams et al., 2014, 2016, 2018a).

287 Changes in calcium (Ca^{2+}) level contribute to the induction of jasmonic acid synthesis as
288 a component of plant defense (Choi et al., 2017; Howe et al., 2018). Toyota et al. (2018) showed
289 that cytosolic calcium levels increased markedly in phloem cells of sink leaves within one or two
290 min after a source leaf was subjected to wounding or herbivory that impacted phloem cells. This
291 finding demonstrates that signaling for induction of jasmonic acid synthesis can be propagated
292 rapidly throughout a plant via the phloem.

293

294 **6. From Sieve Elements to Larger Scales**

295 Sieve elements not only link multiple functions of the leaf and connect the various organs of the
296 whole plant, but could, by extension, also be seen as a nexus for the terrestrial biosphere and
297 humanity (Adams, 2018). Synthesis and distribution of energy-rich compounds throughout the
298 plant provide the basis for primary production in the major terrestrial biomes (Field et al., 1998)
299 as well as in terrestrial agriculture (Weinzettel et al., 2019). In addition, a large fraction of

300 carbon is sequestered in plants and soil (Raven and Karley, 2006) as an important component of
301 the global carbon cycle.

302 Foliar sieve element infrastructure can thus be expected to vary with increases and
303 decreases in primary production in response to contributors to climate change (e.g., rising
304 atmospheric levels of carbon dioxide, elevated temperatures) and their impacts on large-scale
305 phenomena including altered precipitation patterns, rising sea level, forest fires, insect and
306 pathogen outbreaks, etc. and their complex effect on plant productivity. While some of these
307 factors induce increased carbon sequestration by plants (Nemani et al., 2003; Norby et al., 2005;
308 Fu et al., 2018), many result in reduced levels of sequestration and some result in net carbon
309 emission (Cox et al., 2000; Ciais et al., 2005; Olofsson et al., 2011; Rohrs-Richey et al., 2011;
310 Koebsch et al., 2013; Appenzeller, 2015; Björkman and Niemelå, 2015; Han et al., 2015; Hof
311 and Svahlin, 2016; Jones, 2016; Ramsfield et al., 2016; Loehman et al., 2017; Wolton et al.,
312 2017; Wyka et al., 2017; Smart et al., 2020; Enríquez-de-Salamanca, 2020; Witze, 2020; Doyle
313 et al., 2021; Liu et al., 2021; Martinez and Ardón, 2021) that further contributes to the rise in
314 atmospheric carbon dioxide.

315

316 **Author Contributions**

317 WWA: Conceptualization, Visualization, Funding acquisition, Resources, Supervision, Project
318 administration, Writing – Original Draft. JJS: Investigation, Formal analysis, Visualization,
319 Funding acquisition, Writing – Review & Editing. SKP: Investigation, Formal analysis, Writing
320 – Review & Editing. BD-A: Conceptualization, Visualization, Funding acquisition, Resources,
321 Supervision, Project administration, Writing – Original Draft.

322

323 **Funding**

324 This work was supported by the United States National Science Foundation [award numbers
325 IOS-0841546, DEB-1022236, IOS-1907338] and the University of Colorado at Boulder, USA.

326

327 **Conflict of Interest**

328 We declare no conflict of interest.

329

330 **Acknowledgements**

331 Drs. Christopher Cohu and Onno Muller were instrumental in the generation of the original data
332 on which this review is based. We thank Dr. Sean Gleason for valuable discussion.

333

334 **References**

335 Adams, W.W. III, 2018. Preface: the importance of leave to life and humanity, in: Adams III,
336 W.W., Terashima, I. (Eds.), *The Leaf: A Platform for Performing Photosynthesis.*
337 *Advances in Photosynthesis and Respiration*, Volume 44. Springer International
338 Publishing, Cham, pp. xxvii–xxxiv. <https://doi.org/10.1007/978-3-319-93594-2>

339 Adams, W.W. III, Cohu, C.M., Muller, O., Demmig-Adams, B., 2013. Foliar phloem
340 infrastructure in support of photosynthesis. *Front. Plant Sci.* 4, 194.
341 <https://doi.org/10.3389/fpls.2013.00194>

342 Adams, W.W. III, Cohu, C.M., Amiard, V., Demmig-Adams, B., 2014. Associations between
343 phloem-cell wall ingrowths in minor veins and maximal photosynthesis rate. *Front. Plant*
344 *Sci.* 5, 24. <https://doi.org/10.3389/fpls.2014.00024>

345 Adams, W.W. III, Stewart, J.J., Cohu, C.M., Muller, O., Demmig-Adams, B., 2016. Habitat
346 temperature and precipitation of *Arabidopsis thaliana* ecotypes determine the response of
347 foliar vasculature, photosynthesis, and transpiration to growth temperature. *Front. Plant*
348 *Sci.* 7, 1026. <https://doi.org/10.3389/fpls.2016.01026>

349 Adams, W.W. III, Stewart, J.J., Polutchnko, S.K., Demmig-Adams, B., 2018a. Leaf vasculature
350 and the upper limit of photosynthesis, in: Adams III, W.W., Terashima, I. (Eds.), *The Leaf:*
351 *A Platform for Performing Photosynthesis. Advances in Photosynthesis and Respiration*,
352 Volume 44. Springer International Publishing, Cham, pp. 27–54.
353 https://doi.org/10.1007/978-3-319-93594-2_2

354 Adams, W.W. III, Stewart, J.J., Demmig-Adams, B., 2018b. Photosynthetic modulation in
355 response to plant activity and environment, in: Adams III, W.W., Terashima, I. (Eds.), The
356 Leaf: A Platform for Performing Photosynthesis. Advances in Photosynthesis and
357 Respiration, Volume 44. Springer International Publishing, Cham, pp. 493-563.
358 https://doi.org/10.1007/978-3-319-93594-2_18

359 Ali, M.S., Baek, K.-H., 2020. Jasmonic acid signaling pathway in response to abiotic stresses in
360 plants. *Intl. J. Mol. Sci.* 21, 621. <https://doi.org/10.3390/ijms21020621>

361 Amiard, V., Mueh, K.E., Demmig-Adams, B., Ebbert, V., Turgeon, R., Adams, W.W. III, 2005.
362 Anatomical and photosynthetic acclimation to the light environment in species with
363 differing mechanisms of phloem loading. *Proc. Natl. Acad. Sci. U.S.A.* 102, 12968-12973
364 <https://doi.org/10.1073/pnas.0503784102>

365 Amiard, V., Demmig-Adams, B., Mueh, K.E., Turgeon, R., Combs, A.F., Adams, W.W. III,
366 2007. Role of light and jasmonic acid signaling in regulating foliar phloem cell wall
367 ingrowth development. *New Phytol.* 173, 722-731. <https://doi.org/10.1111/j.1469-8137.2006.01954.x>

369 Appenzeller, T., 2015. The new North – stoked by climate change, fire and insects are remaking
370 the planet's vast boreal forest. *Science* 349, 806-809.
371 <https://doi.org/10.1126/science.349.6250.806>

372 Ayre, B.G., Turgeon, R., 2018. Export of photosynthates from the leaf, in: Adams III, W.W.,
373 Terashima, I. (Eds.), The Leaf: A Platform for Performing Photosynthesis. Advances in
374 Photosynthesis and Respiration, Volume 44. Springer International Publishing, Cham, pp.
375 27–54. https://doi.org/10.1007/978-3-319-93594-2_3

376 Babst, B.A., Gao, F., Acosta-Gamboa, L.M., Karve, A., Schueller, M.J., Lorence, A., 2019.
377 Three *NPF* genes in *Arabidopsis* are necessary for normal nitrogen cycling under low
378 nitrogen stress. *Plant Physiol. Biochem.* 143, 1-10.
379 <https://doi.org/10.1016/j.plaphy.2019.08.014>

380 Barunawati, N., Hettwer Giehl, R.F., Bauer, B., von Wirén, N., 2013. The influence of inorganic
381 nitrogen fertilizer forms on micronutrient retranslocation and accumulation in grains of
382 winter wheat. *Front. Plant Sci.* 4, 320. <https://doi.org/10.3389/fpls.2013.00320>

383 Björkman, C., Niemelå, P., 2015. Climate change and insect pests. CABI Publishing,
384 Wallingford

385 Bohner, A., Kojima, S., Hajirezaei, M., Melzer, M., von Wirén, N., 2014. Urea retranslocation
386 from senescing *Arabidopsis* leaves is promoted by DUR3-mediated urea retrieval from leaf
387 apoplast. *Plant J.* 81, 377-387. <https://doi.org/10.1111/tpj.12740>

388 Brodribb, T.J., Buckley, T.N., 2018. Leaf water transport: a core system in the evolution and
389 physiology of photosynthesis, in: Adams III, W.W., Terashima, I. (Eds.), The Leaf: A
390 Platform for Performing Photosynthesis. Springer International Publishing, Advances in
391 Photosynthesis and Respiration, Volume 44. Cham, pp. 27–54. https://doi.org/10.1007/978-3-319-93594-2_4

393 Carvalho, M.R., Losada, J.M., Niklas, K.J., 2018. Phloem networks in leaves. *Curr. Opin. Plant*
394 *Biol.* 43, 29-35. <https://doi.org/10.1016/j.pbi.2017.12.007>

395 Chen, L.-Q., Qu, X.-Q., Hou, B.-H., Sosso, D., Osorio, S., Fernie, A.R., Frommer, W.B., 2012.
396 Sucrose efflux mediated by SWEET proteins as a key step for phloem transport. *Science*
397 335, 207-211. <https://doi.org/10.1126/science.1213351>

398 Choi, W.-G., Miller, G., Wallace, I., Harper, J., Mittler, R., Gilroy, S., 2017. Orchestrating rapid
399 long-distance signaling in plants with Ca^{2+} , ROS and electrical signals. *Plant J.* 90, 698-
400 707. <https://doi.org/10.1111/tpj.13492>

401 Ciais, P., Reichstein, M., Viovy, N., Granier, A., Ogée, J., Allard, V., Aubinet, M., Buchmann,
402 N., Bernhofer, C., Carrara, A., Chevallier, R., De Noblet, N., Friend, A.D., Friedlingstein,
403 P., Grimwald, T., Heinesch, B., Kersten, P., Knohl, A., Krinner, G., Loustau, D., Manca,
404 G., Matteucci, G., Miglietta, F., Ourcival, J.M., Papale, D., Pilegaard, K., Rambal, S.,
405 Seufert, G., Soussana, J.F., Sanz, M.J., Schulze, E.D., Vesala, T., Valentini, R. 2005.
406 Europe-wide reduction in primary productivity caused by the heat and drought in 2003.
407 *Nature* 437, 529-533. <https://doi.org/10.1038/nature03972>

408 Cohu, C.M., Muller, O., Demmig-Adams, B., Adams, W.W. III, 2013a. Minor loading vein
409 acclimation for three *Arabidopsis thaliana* ecotypes in response to growth under different
410 temperature and light regimes. *Front. Plant Sci.* 4, 240.
411 <https://doi.org/10.3389/fpls.2013.00240>

412 Cohu, C.M., Muller, O., Stewart, J.J., Demmig-Adams, B., Adams, W.W. III, 2013b.
413 Association between minor loading vein architecture and light- and CO_2 -saturated rates of
414 photosynthetic oxygen evolution among *Arabidopsis thaliana* ecotypes from different
415 latitudes. *Front. Plant Sci.* 4, 264. <https://doi.org/10.3389/fpls.2013.00264>

416 Cohu, C.M., Muller, O., Adams, W.W. III, Demmig-Adams, B., 2014. Leaf anatomical and
417 photosynthetic acclimation to cool temperature and high light in two winter versus two
418 summer annuals. *Physiol. Plant.* 152, 164-173. <https://doi.org/10.1111/ppl.12154>

419 Cox, P.M., Betts, R.A., Jones, C.D., Spall, S.A., Totterdell, I.J., 2000. Acceleration of global
420 warming due to carbon-cycle feedbacks in a coupled climate model. *Nature* 408, 184-187.
421 <https://doi.org/10.1038/35041539>

422 de Boer, H.J., Drake, P.L., Wendt, E., Price, C.A., Schulze, E.-D., Turner, N.C., Nicolle, D.,
423 Veneklaas, E.J., 2016. Apparent overinvestment in leaf venation relaxes leaf morphological
424 constraints on photosynthesis in arid habitats. *Plant Physiol.* 172, 2286-2299.
425 <https://doi.org/10.1104/pp.16.01313>

426 Demmig-Adams, B., Cohu, C.M., Amiard, V., van Zadelhoff, G., Veldink, G.A., Muller, O.,
427 Adams, W.W. III, 2013. Emerging trade-offs – impact of photoprotectants (PsbS,
428 xanthophylls, and vitamin E) on oxylipins as regulators of development and defense. *New*
429 *Phytol.* 197, 720-729. <https://doi.org/10.1111/nph.12100>

430 Demmig-Adams, B., Stewart, J.J., Burch, T.A., Adams, W.W. III, 2014a. Insights from placing
431 photosynthetic light harvesting into context. *J. Phys. Chem. Lett.* 5, 2880-2889.
432 <https://doi.org/10.1021/jz5010768>

433 Demmig-Adams, B., Stewart, J.J., Adams, W.W. III 2014b. Chloroplast photoprotection and the
434 trade-off between abiotic and biotic defense, in: Demmig-Adams, B., Garab, G., Adams,
435 W.W. III, Govindjee (Eds.) *Non-Photochemical Quenching and Energy Dissipation in*

436 Plants, Algae and Cyanobacteria. *Advances in Photosynthesis and Respiration*, Volume
437 40. Springer, Dordrecht, pp. 631-643. https://doi.org/10.1007/978-94-017-9032-1_28

438 Demmig-Adams, B., Stewart, J.J., Adams, W.W. III, 2017. Environmental regulation of intrinsic
439 photosynthetic capacity: An integrated view. *Curr. Opin. Plant Biol.* 37, 34-41.
440 <https://doi.org/10.1016/j.pbi.2017.03.008>

441 Demmig-Adams, B., Stewart, J.J., Baker, C.R., Adams, W.W. III, 2018. Optimization of
442 photosynthetic productivity in contrasting environments by regulons controlling plant form
443 and function. *Intl. J. Mol. Sci.* 19, 872. <https://doi.org/10.3390/ijms1903872>

444 Doyle, J.M., Earley, K.E., Atkinson, R.B., 2021. An analysis of Atlantic white cedar
445 (*Chamaecyparis thyoides* (L.) B.S.P) tree rings as indicators of ghost forest development in
446 a globally threatened ecosystem. *Forests* 12, 973. <https://doi.org/10.3390/f12080973>

447 Duan, Z., Homma, A., Kobayashi, M., Nagata, N., Kaneko, Y., Fujiki, Y., Nishida, I., 2014.
448 Photoassimilation, assimilate translocation and plasmodesmal biogenesis in the source
449 leaves of *Arabidopsis thaliana* grown under an increased atmospheric CO₂ concentration.
450 *Plant Cell Physiol.* 55, 358-369. <https://doi.org/10.1093/pcp.pcu004>

451 Dumlaor, M.R., Darehshouri, A., Cohu, C.M., Muller, O., Mathias, J., Adams, W.W. III,
452 Demmig-Adams, B., 2012. Low temperature acclimation of photosynthetic capacity and
453 leaf morphology in the context of phloem loading type. *Photosynth. Res.* 113, 181-189
454 <https://doi.org/10.1007/s11120-012-9762-5>

455 Dunbar-Co, S., Sporck, M.J., Sack, L., 2009. Leaf trait diversification and design in seven rare
456 taxa of the Hawaiian *Plantago* radiation. *Intl. J. Plant Sci.* 170, 61-75.
457 <https://doi.org/10.1086/59311>

458 Durand, M., Porcheron, B., Hennion, N., Maurousset, L., Lemoine, R., Pourtau, N., 2016. Water
459 deficit enhances C export to the roots in *Arabidopsis thaliana* plants with contribution of
460 sucrose transporters in both shoot and roots. *Plant Physiol.* 170, 1460-1479.
461 <https://doi.org/10.1104/pp.15.01926>

462 Enríquez-de-Salamanca, Á., 2020. Contribution to climate change of forest fires in Spain:
463 emissions and loss of sequestration. *J. Sust. Forest.* 39, 417-431.
464 <https://doi.org/10.1080/10549811.2019.1673779>

465 Eom, J.-S., Chen, L.-Q., Sosso, D., Julius, B.T., Lin, I.W., Qu, X.-Q., Braun, D.M., Frommer,
466 W.B., 2015. SWEETs, transporters for intracellular and intercellular sugar translocation.
467 *Curr. Opin. Plant Biol.* 25, 53-62. <https://doi.org/10.1016/j.pbi.2015.04.005>

468 Esau, K., 1977. *Anatomy of Seed Plants*, 2nd Edition. John Wiley and Sons, New York

469 Falhof, J., Pedersen, J.T., Fuglsang, A.T., Palmgren, M., 2016. Plasma membrane H⁺-ATPase
470 regulation in the center of plant physiology. *Mol. Plant* 9, 323-337.
471 <https://doi.org/10.1016/j.molp.2015.11.002>

472 Fellows, R.J., Geiger, D.R., 1974. Structural and physiological changes in sugar beet leaves
473 during sink to source conversion. *Plant Physiol.* 54, 877-885.
474 <https://doi.org/10.1104/pp.54.6.877>

475 Field, C.B., Behrenfeld, M.J., Randerson, J.T., Falkoski, P., 1998. Primary production of the
476 biosphere: integrating terrestrial and oceanic components. *Science* 281, 237-240.
477 <https://doi.org/10.1126/science.281.5374.237>

478 Fondy, B.R., Geiger, D.R., 1982. Diurnal pattern of translocation and carbohydrate metabolism
479 in source leaves of *Beta vulgaris* L. *Plant Physiol.* 70, 671-676.
480 <https://doi.org/10.1104/pp70.3.671>

481 Foyer, C.H., Noctor, G., 2009. Redox regulation in photosynthetic organisms: signaling,
482 acclimation, and practical implications. *Antioxid. Redox Signal.* 11, 861-905.
483 <https://doi.org/10.1089/ars.2008.2177>

484 Fu, Y.H., Piao, S., Delpierre, N., Hao, F., Hänninen, H., Liu, Y., Sun, W., Janssens, I.A.,
485 Campioli, M., 2018. Larger temperature response of autumn leaf senescence than spring
486 leaf-out phenology. *Glob. Chang. Bio.* 24, 2159-2168. <https://doi.org/10.1111/gcb.14021>

487 Gagnon, M.-J., Beebe, D.U., 1996. Establishment of a plastochnon index and analysis of the
488 sink-to-source transition in leaves of *Moricandia arvensis* (L.) DC. (Brassicaceae). *Intl. J.
489 Plant Sci.* 167, 262-268. <https://doi.org/10.1086/297345>

490 Gaufichon, L., Masclaux-Daubresse, C., Tcherkez, G., Reisdorf-Cren, M., Sakakibara, Y., Hase,
491 T., Clément, G., Avice, J.-C., Grandjean, O., Marmagne, A., Boutet-Mercey, S., Azzopardi,
492 M., Soulay, F., Suzuki, A., 2013. *Arabidopsis thaliana ASN2* encoding asparagine
493 synthetase is involved in the control of nitrogen assimilation and export during vegetative
494 growth. *Plant Cell Environ.* 36, 328-342. [https://doi.org/10.1111/j.1365-3040.2012.02576.x](https://doi.org/10.1111/j.1365-
495 3040.2012.02576.x)

496 Gaxiola, R.A., Palmgren, M.G., Schumacher, K., 2007. Plant proton pumps. *FEBS Lett.* 581,
497 2204-2214. <https://doi.org/10.1016/j.febslet.2007.03.050>

498 Han, G., Chu, X., Xing, Q., Li, D., Yu, J., Luo, Y., Wang, G., Mao, P., Rafique, R., 2015. Effects
499 of episodic flooding on the net ecosystem CO₂ exchange of a supratidal wetland in the
500 Yellow River Delta. *J. Geophys. Res. Biogeosci.* 120, 1506-1520.
501 <https://doi.org/10.1002/2015JG002923>

502 Haritatos, E., Medville, R., Turgeon, R., 2000. Minor vein structure and sugar transport in
503 *Arabidopsis thaliana*. *Planta* 211, 105-111. <https://doi.org/10.1007/s004250000268>

504 Hause, B., Hause, G., Kutter, C., Miersch, O., Wasternack, C., 2003. Enzymes of jasmonate
505 biosynthesis occur in tomato sieve elements. *Plant Cell Physiol.* 44, 643-648.
506 <https://doi.org/10.1093/pcp/pcg072>

507 Hesse, B.D., Goisser, M., Hartmann, H., Grams, T.E.E., 2019. Repeated summer drought delays
508 sugar export from the leaf and impairs phloem transport in mature beech. *Tree Physiol.* 39,
509 192-200. <https://doi.org/10.1093/treephys/tpy122>

510 Hof, A.R., Svahlin, A., 2016. The potential effect of climate change on the geographical
511 distribution of insect pest species in the Swedish boreal forest. *Scand. J. For. Res.* 31, 29-
512 39. <https://doi.org/10.1080/02827581.2015.1052751>

513 Howe, G.A., Major, I.T., Koo, A.J., 2018. Modularity in jasmonate signaling for multistress
514 resilience. *Annu. Rev. Plant Biol.* 69, 387-415. [https://doi.org/10.1146/annurev-arplant-042817-040047](https://doi.org/10.1146/annurev-arplant-
515 042817-040047)

516 Hölttä, T., Vesala, T., Sevanto, S., Perämäki, M., Nikinmaa, E. 2006. Modeling xylem and
517 phloem flows in trees according to cohesion theory and Münch hypothesis. *Trees* 20, 67-
518 78. <https://doi.org/10.1007/s00468-005-0014-6>

519 Hüner, N.P.A., Dahal, K., Bode, R., Kurepin, L.V., Ivanov, A.G., 2016. Photosynthetic
520 acclimation, vernalization, crop productivity and ‘the grand design of photosynthesis’. *J.*
521 *Plant Physiol.* 203, 29-43. <https://doi.org/10.1016/j.jplph.2016.04.006>

522 Ishihara, H., Moraes, T.A., Pyl, E.-T., Schulze, W.X., Obata, T., Scheffel, A., Fernie, A.R.,
523 Sulpice, R., Stitt, M., 2017. Growth rate correlates negatively with protein turnover in
524 *Arabidopsis* accessions. *Plant J.* 91, 416-429. <https://doi.org/10.1111/tpj.13576>

525 Jeong, K., Baten, A., Waters, D.L.E., Pantoja, O., Julia, C.C., Wissuwa, M., Jeuer, S.,
526 Kretzschmar, T., Rose, T.J., 2017. Phosphorus remobilization from rice flag leaves during
527 grain filling: an RNA-seq study. *Plant Biotech. J.* 15, 15-26.
528 <https://doi.org/10.1111/pbi.12586>

529 Jeschke, W.D., Pate, J.S., 1995. Mineral nutrition and transport in xylem and phloem of *Banksia*
530 *prionotes* (Proteaceae), a tree with dimorphic root morphology. *J. Exp. Bot.* 46, 895-905.
531 <https://doi.org/10.1093/jxb/46.8.895>

532 Jones, R.A.C., 2016. Future scenarios for plant virus pathogens as climate change progresses, in:
533 Kielian, M., Maramorosch, K., Mettenleiter, T.C. (Eds.) *Advances in Virus Research*,
534 Volume 95, Elsevier, San Diego, pp. 87-147. <https://doi.org/10.1016/bs.aivir.2016.02.004>

535 Khan, R.I., Choudhuri, M.A., 1992. Influence of reproductive organs on plant senescence in rice
536 and wheat. *Biol. Plant.* 34, 241-251. doi: 10.1007/BF02925876

537 Koebisch, R., Glatzel, S., Hofmann, J., Forbrich, I., Jurasiczki, G., 2013. CO₂ exchange of a
538 temperate fen during the conversion from moderately rewetting to flooding. *J. Geophys.*
539 *Res. Biogeosci.* 118, 940-950. <https://doi.org/10.1002/jgrg.20069>

540 Koenig, A.M., Hoffmann-Benning, S., 2020. The interplay of phloem-mobile signals in plant
541 development and stress response. *Biosci. Rep.* 40, BSR20193329.
542 <https://doi.org/10.1042/BSR20193329>

543 Leister, D., 2019. Piecing the puzzle together: the central role of reactive oxygen species and
544 redox hubs in chloroplast retrograde signaling. *Antiox. Redox Signal.*
545 <https://doi.org/10.1089/ars.2017.7392>

546 Liu, X., He, B., Guo, L., Huang, L., Yuan, W., Chen, X., Hao, X., Xie, X., Zhang, Y., Zhong, Z.,
547 Li, T., Chen, A., 2021. European carbon uptake has not benefited from vegetation greening.
548 *Geophys. Res. Lett.* 48, e2021GL094870. <https://doi.org/10.1029/2021GL094870>

549 Loehman, R.A., Keane, R.E., Hollsinger, L.M., Wu, Z., 2017. Interactions of landscape
550 disturbances and climate change dictate ecological pattern and process: spatial modeling of
551 wildfire, insect, and disease dynamics under future climates. *Landsc. Ecol.* 32, 1447-1459.
552 <https://doi.org/10.1007/s10980-016-0414-6>

553 Martinez, M., Ardón, M., 2021. Drivers of greenhouse gas emissions from standing dead trees in
554 ghost forests. *Biogeochemistry* 154, 471-488. <https://doi.org/10.1007/s10533-021-00797-5>

555 Mengin, V., Pyl, E.-T., Moraes, T.A., Sulpice, R., Encke, B., Stitt, M., 2017. Photosynthate

partitioning to starch in *Arabidopsis thaliana* is insensitive to light intensity but sensitive to photoperiod due to a restriction on growth in the light in short photoperiods. *Plant Cell Environ.* 40, 2608-2627. <https://doi.org/10.1111/pce.13000>

Muller, O., Cohu, C.M., Stewart, J.J., Protheroe, J.A., Demmig-Adams, B., Adams, W.W. III, 2014a. Association between photosynthesis and contrasting features of minor veins in leaves of summer annuals loading phloem via symplastic versus apoplastic routes. *Physiol. Plant.* 152, 174-183. <https://doi.org/10.1111/ppl.12155>

Muller, O., Stewart, J.J., Cohu, C.M., Polutchko, S.K., Demmig-Adams, B., Adams, W.W. III, 2014b. Leaf architectural, vascular and photosynthetic acclimation to temperature in two biennials. *Physiol. Plant.* 152, 763-772. <https://doi.org/10.1111/ppl.12226>

Nemani, R.R., Keeling, C.D., Hashimoto, H., Jolly, W.M., Piper, S.C., Tucker, C.J., Myneni, R.B., Running, S.W., 2003. Climate-driven increases in global terrestrial net primary production from 1982 to 1999. *Science*, 300, 1560-1563. <https://doi.org/10.1126/science.1082750>

Nikinmaa, E., Hölttä, T., Hari, P., Kolari, P., Mäkelä, A., Sevanto, S., Vesala, T., 2013. Assimilate transport in phloem sets conditions for leaf gas exchange. *Plant Cell Environ.* 36, 655-669. <https://doi.org/10.1111/pce.12004>

Ninan, A.S., Grant, J., Song, J., Jameson, P.E., 2019. Expression of genes related to sugar and amino acid transport and cytokinin metabolism during leaf development and senescence in *Pisum sativum* L. *Plants* 8, 76. <https://doi.org/10.3390/plants8030076>

Ning, P., Li, S., Yu, P., Zhang, Y., Li, C., 2013. Post-silking accumulation and partitioning of dry matter, nitrogen, phosphorus and potassium in maize varieties differing in leaf longevity. *Field Crops Res.* 144, 19-27. <https://doi.org/10.1016/j.fcr.2013.01.020>

Norby, R.J., DeLucia, E.H., Gielen, B., Calfapietra, C., Giardina, C.P., King, J.S., Ledford, J., McCarthy, H.R., Moore, D.J.P., Ceulemans, R., De Angelis, P., Finzi, A.C., Karnosky, D.F., Kubiske, M.E., Lukac, M., Pregitzer, K.S., Scarascia-Mugnozza, G.E., Schlesdinger, W.H., Oren, R., 2005. Forest response to elevated CO₂ is conserved across a broad range of productivity. *Proc. Natl. Acad. Sci. U.S.A.* 102, 18052-18056. <https://pnas.org/cgi/doi/pnas.0509478102>

Offler, C.E., McCurdy, D.W., Patrick, J.W., Talbot, M.J., 2003. Transfer cells: cells specialized for a special purpose. *Annu. Rev. Plant Biol.* 54, 431-454. <https://doi.org/10.1146/annurev.arplant.54.031902.134812>

Olofsson, J., Ericson, L., Torp, M., Stark, S., Baxter, R., 2011. Carbon balance of Arctic tundra under increased snow cover mediated by a plant pathogen. *Nature Clim. Change* 1, 220-223. <https://doi.org/10.1038/nclimate1142>

Pearce, S., Tabbita, F., Cantu, D., Buffalo, V., Avni, R., Vazquez-Gross, H., Zhao, R., Conley, C.J., Distelfeld, A., Dubcovksy, J., 2014. Regulation of Zn and Fe transporters by the *BPC1* gene during early wheat monocarpic senescence. *BMC Plant Biol.* 14, 368. <https://doi.org/10.1186/s12870-014-0368-2>

Pérez-Alonso, M.-M., Sánchez-Parra, B., Ortiz-García, P., Santamaría, M.E., Díaz, I., Pollmann, S., 2021. Jasmonic acid-dependent MYC transcription factors bind to a tandem G-box

597 motif in the YUCCA8 and YUCCA9 promoters to regulate biotic stress responses. *Intl. J.*
598 *Mol. Sci.* 22, 9768. <https://doi.org/10.3390/ijms22189768>

599 Piirainen, M., Liebisch, O., Kadereit, G., 2017. Phylogeny, biogeography, systematics and
600 taxonomy of Salicornioideae (Amaranthaceae/Chenopodiaceae) – a cosmopolitan, highly
601 specialized hydrohalophyte lineage dating back to the Oligocene. *Taxon* 66, 109-132.
602 <https://doi.org/10.12705/661.6>

603 Polutchko, S.K., Stewart, J.J., Adams, W.W. III, Demmig-Adams, B., 2021. Photosynthesis and
604 foliar vascular adjustments to growth light intensity in summer annual species with
605 symplastic and apoplastic phloem loading. *J. Plant Physiol.* 267, 153532.
606 <https://doi.org/10.1016/j.jplph.2021.153532>

607 Ramsfield, T.D., Bentz, B.J., Faccoli, M., Jactel, H., Brockerhoff, E.G., 2016. Forest health in a
608 changing world: effects of globalization and climate change on forest insect and pathogen
609 impacts. *Forestry* 89, 245-252. <https://doi.org/10.1093/forestry/cpw018>

610 Raven, J.A., Karley, A.J., 2006. Carbon sequestration: photosynthesis and subsequent processes.
611 *Curr. Biol.* 16, R165-R167. <https://doi.org/10.1016/j.cub.2006.02.041>

612 Rennie, E.A., Turgeon, R., 2009. A comprehensive picture of phloem loading strategies. *Proc.*
613 *Natl. Acad. Sci. U.S.A.* 106, 14162-14167. <https://doi.org/10.1073/pnas.0902279106>

614 Rohrs-Richey, J.K., Mulder, C.P.H., Winton, L.M., Stanosz, G., 2011. Physiological
615 performance of an Alaskan shrub (*Alnus fruticosa*) in response to disease (*Valsa*
616 *melanodiscus*) and water stress. *New Phytol.* 189, 295-307. <https://doi.org/10.1111/j.1469-8137.2010.03472.x>

618 Römhild, V., Schaaf, G., 2004. Iron transport in plants: future research in view of a plant
619 nutritionist and a molecular biologist. *Soil Sci. Plant Nutr.* 50, 1003-1012.
620 <https://doi.org/10.1080/00380768.2004.10408567>

621 Sample, R., Babst, B.A., 2019. Timing of nitrogen resorption-related processes during fall
622 senescence in southern oak species. *For. Sci.* 65, 245-249.
623 <https://doi.org/10.1093/forsci/fxy062>

624 Schippers, J.H.M., Foyer, C.H., van Dongen, J.T., 2016. Redox regulation in shoot growth, SAM
625 maintenance and flowering. *Curr. Opin. Plan Biol.* 29, 121-128.
626 <https://doi.org/10.1016/j.pbi.2015.11.009>

627 Schleucher, J., Vanderveer, P.J., Sharkey, T.D., 1998. Export of carbon from chloroplasts at
628 night. *Plant Physiol.* 118, 1439-1445. <https://doi.org/10.1104/pp.118.4.1439>

629 Schmalstig, J.G., Geiger, D.R., 1987. Phloem unloading in developing leaves of sugar beet. II.
630 Termination of phloem unloading. *Plant Physiol.* 83, 49-52.
631 <https://doi.org/10.1104/pp.83.1.49>

632 Sharkey, T.D., 2017. A dichotomy resolved: plant growth can control the rate of starch
633 accumulation. *Plant Cell Environ.* 40, 2602-2607. <https://doi.org/10.1111/pce.13059>

634 Shi, R., Bäßler, R., Zou, C., Römhild, V., 2011. Is iron phloem mobile during senescence in
635 trees? A reinvestigation of Rissmüller's finding of 1874. *Plant Physiol. Biochem.* 49, 489-
636 493. <https://doi.org/10.1016/j.plaphy.2011.03.004>

637 Shi, R., Weber, G., Köster, J., Reza-Hajirezaei, M., Zou, C., Zhang, F., von Wirén, N., 2012.
638 Senescence-induced iron mobilization in source leaves of barley (*Hordeum vulgare*) plants.
639 *New Phytol.* 195, 372-383. <https://doi.org/10.1111/j.1469-8137.2012.04165.x>

640 Slewinski, T.L., Zhang, C., Turgeon, R., 2013. Structural and functional heterogeneity in phloem
641 loading and transport. *Front. Plant Sci.* 4, 244. <https://doi.org/10.3389/fpls.2013.00244>

642 Smart, L.S., Taillie, P.J., Poulter, B., Vukomanovic, J., Singh, K.K., Swenson, J.J., Mitasova, H.,
643 Smith, J.W., Meentemeyer, R.K., 2020. Aboveground carbon loss associated with the
644 spread of ghost forests as sea levels rise. *Environ. Res. Lett.* 15, 104028.
645 <https://doi.org/10.1088/1748-9326/aba136>

646 Sondergaard, T.E., Schulz, A., Palmgren, M.G., 2004. Energization of transport processes in
647 plants. Roles of the plasma membrane H⁺-ATPase. *Plant Physiol.* 136, 2475-2482.
648 <https://doi.org/10.1104/pp.104.048231>

649 Srivastava, A.C., Ganesan, S., Ismail, I.O., Ayre, B.G., 2008. Functional characterization of the
650 *Arabidopsis* AtSUC2 sucrose/H⁺ symporter by tissue-specific complementation reveals an
651 essential role in phloem loading but not in long-distance transport. *Plant Physiol.* 148, 200-
652 211. <https://doi.org/10.1104/pp.108.124776>

653 Srivastava, A., Redij, T., Sharma, B., 2017. Interaction between hormone and redox signaling in
654 plants: divergent pathways and convergent roles, in: Pandey, G.K. (Ed.) *Mechanisms of*
655 *Plant Hormone Signaling under Stress*, II, John Wiley & Sons, Inc., Hoboken, NJ, pp. 1-22.
656 <https://doi.org/10.1002/9781118889022.ch19>

657 Stewart, J.J., Demmig-Adams, B., Cohu, C.M., Wenzl, C.A., Muller, O., Adams W.W. III, 2016.
658 Growth temperature impact on leaf form and function in *Arabidopsis thaliana* ecotypes
659 from northern and southern Europe. *Plant Cell Environ.* 39, 1549-1558.
660 <https://doi.org/10.1111/pce.12720>

661 Stewart, J.J., Polutchko, S.K., Adams, W.W. III, Demmig-Adams, B., 2017a. Acclimation of
662 Swedish and Italian ecotypes of *Arabidopsis thaliana* to light intensity. *Photosynth. Res.*
663 134, 215-229. <https://doi.org/10.1007/s11120-017-0436-1>

664 Stewart, J.J., Polutchko, S.K., Adams, W.W. III, Cohu, C.M., Wenzl, C.A., Demmig-Adams, B.,
665 2017b. Light, temperature and tocopherol status influence foliar vascular anatomy and leaf
666 function in *Arabidopsis thaliana*. *Physiol. Plant.* 160, 98-110.
667 <https://doi.org/10.1111/ppl.12543>

668 Stewart, J.J., Muller, O., Cohu, C.M., Demmig-Adams, B., Adams, W.W. III, 2019.
669 Quantification of leaf phloem anatomical features with microscopy, in: Liesche, J. (Ed.),
670 *Phloem: Methods and Protocols*. Springer, New York, NY, pp. 55-72.
671 https://doi.org/10.1007/978-1-4939-9562-2_5

672 Tegeder, M., Hammes, U.Z., 2018. The way out and in: phloem loading and unloading of amino
673 acids. *Curr. Opin. Plant Biol.* 43, 16-21. <https://doi.org/10.1016/j.pbi.2017.12.002>

674 Tegeder, M., Masclaux-Daubresse, C., 2018. Source and sink mechanisms of nitrogen transport
675 and use. *New Phytol.* 217, 35-53. <https://doi.org/10.1111.nph.14876>

676 Toyota, M., Spencer, D., Sawai-Toyota, S., Jiaqi, W., Zhang, T., Koo, A.J., Howe, G.A., Gilroy,
677 S., 2018. Glutamate triggers long-distance, calcium-based plant defense signaling. *Science*
678 361, 1112-1115. <https://doi.org/10.1126/science.aat7744>

679 Turgeon, R., 1989. The sink-source transition in leaves. *Annu. Rev. Plant Physiol. Plant Mol.*
680 *Biol.* 40, 119-138. <https://doi.org/10.1146/annurev.pp.40.060189.001003>

681 Turgeon, R., 2006. Phloem loading: how leaves gain their independence. *BioScience* 56, 15-24,
682 [https://doi.org/10.1641/0006-3568\(2006\)056\[0015:PLHLGT\]2.0.CO;2](https://doi.org/10.1641/0006-3568(2006)056[0015:PLHLGT]2.0.CO;2)

683 Turgeon, R., Webb, J.A., 1973, Leaf development and phloem transport in *Cucurbita pepo*:
684 transition from import to export. *Planta* 113, 179-191. <https://doi.org/10.1007/BF00388202>

685 Unal, D., García-Caparrós, P., Kumar, V., Dietz, K.-J., 2020. Chloroplast-associated molecular
686 patterns as concept for fine-tuned operational retrograde signalling. *Phil. Trans. R. Soc. B.*
687 375, 2019.0443. <https://doi.org/10.1098/rstb.2019.0443>

688 van Bel, A.J.E., 1990. Xylem-phloem exchange via the rays – the undervalued route of transport.
689 *J. Exp. Bot.* 41, 631-644. <https://doi.org/10.1093/jxb/41.6.631>

690 van Bel, A.J.E., 2003. The phloem, a miracle of ingenuity. *Plant Cell Environ.* 26, 125-149.
691 <https://doi.org/10.1046/j.1365-3040.2003.00963.x>

692 Wang, X.-D., Canny, M.J., 1985. Loading and translocation of assimilate in the fine veins of
693 sunflower leaves. *Plant Cell Environ.* 8, 669-685. <https://doi.org/10.1111/1365-3040.ep11611718>

695 Weinzettel, J., Vackárû, D., Medková, H., 2019. Potential net primary production footprint of
696 agriculture: a global trade analysis. *J. Indus. Ecol.* 23, 1133-1142.
697 <https://doi.org/10.1111/jiec.12850>

698 Weise, S.E., Weber, A.P.M., Sharkey, T.D., 2003. Maltose is the major form of carbon exported
699 from the chloroplast at night. *Planta* 218, 474-482. <https://doi.org/10.1007/s00425-003-1128-y>

701 Witze, A., 2020. The Arctic is burning like never before – and that's bad news for climate
702 change. *Nature* 585, 336-337. <https://doi.org/10.1038/d41586-020-02568-y>

703 Wolton, B.M., Flannigan, M.D., Marshall, G.A., 2017. Potential climate change impacts on fire
704 intensity and key wildfire suppression thresholds in Canada. *Environ. Res. Lett.* 12,
705 095003. <https://doi.org/10.1088/1748-9326/aa7e6e>

706 Wyka, S.A., Smith, C., Munck, I.A., Rock, B.N., Ziniti, B.L., Broders, K., 2017. Emergence of
707 white pine needle damage in the northeastern United States is associated with changes in
708 pathogen pressure in response to climate change. *Glob. Chang. Biol.* 23, 394-405.
709 <https://doi.org/10.1111/gcb.13359>

710 Zhang, C., Turgeon, R., 2018. Mechanisms of phloem loading. *Curr. Opin. Plant Biol.* 43, 71-75.
711 <https://doi.org/10.1016/j.pbi.2018.01.009>

712 **Figure Legends**

713 Fig. 1. Light microscopic images of minor vein cross sections from leaves of (A) sunflower
714 (*Helianthus annuus* L. cv. Soraya) and (B) *Arabidopsis thaliana* (L. Heynh. Columbia-0) that
715 developed under $1000 \mu\text{mol photons m}^{-2} \text{ s}^{-1}$ (9-h photoperiod) at leaf temperatures of 25–27°C
716 (and 20°C during the night). In each image, a blue arrow indicates the location of a tracheary
717 element (one of two in the sunflower vein and one of five in the *A. thaliana* vein), a dark green
718 arrow indicates the location of a sieve element (one of two in the sunflower vein and one of eight
719 in the *A. thaliana* vein), and the light green arrows point to a companion cell (CC) and a phloem
720 parenchyma cell (PC) in each image. For details concerning the preparation and analysis of such
721 cross sections, see Stewart et al. (2019; see also Cohu et al., 2014).

722

723 Fig. 2. Relationship between photosynthetic capacity and (A,C) cell number per minor vein \times
724 minor vein density (VD) and (B,D) cell volume per leaf area of (A,B) sieve elements and (C,D)
725 tracheary elements in leaves of *Arabidopsis thaliana* (green symbols) and/or sunflower
726 (*Helianthus annuus*; orange symbols). The characterized minor veins constituted the third and
727 fourth order in leaves of *A. thaliana* and the sixth and seventh order in leaves of sunflower. Both
728 species were grown under four different growth regimes of 400 or $1000 \mu\text{mol photons m}^{-2} \text{ s}^{-1}$ (9-
729 h photoperiod) at leaf temperatures of 25–27°C or 14–16°C (and 20°C or 12.5°C, respectively,
730 during the night). Additionally, *A. thaliana* was grown under 100 or $1000 \mu\text{mol photons m}^{-2} \text{ s}^{-1}$
731 (9-h photoperiod) at a leaf temperature of 20°C (and 12°C at night), and sunflower was grown
732 under 100 and $750 \mu\text{mol photons m}^{-2} \text{ s}^{-1}$ (12-h photoperiod) at a leaf temperature of 27–28°C
733 (and 22°C at night). Data from Cohu et al. (2013a,b, 2014), Adams et al. (2016, 2018a), Stewart
734 et al. (2017a,b), and Polutchnko et al. (2018, 2021). Lines of fit with shaded 95% confidence

735 intervals for (A,D) *A. thaliana* (green lines and shading) and sunflower (orange lines and
736 shading) separately or (B,C) combined (black lines and gray shading).

737

738 Fig. 3. Relationship between leaf thickness and sieve element (A) cross-sectional area per minor
739 vein and (B) cell number per minor vein \times minor vein density (VD) in leaves of *Arabidopsis*
740 *thaliana* (green symbols), sunflower (*Helianthus annuus*; orange symbols), and spinach
741 (*Spinacia oleracea*; dark green symbols). In spinach, the characterized minor veins constituted
742 the fourth and fifth order veins. All species were grown under four different growth regimes of
743 400 or 1000 $\mu\text{mol photons m}^{-2} \text{s}^{-1}$ (9-h photoperiod) at leaf temperatures of 25–27°C or 14–16°C
744 (and 20°C or 12.5°C, respectively, during the night). See the legend of Fig. 2 for additional
745 details regarding the minor veins characterized in sunflower and *A. thaliana* as well as additional
746 growth conditions for *A. thaliana*. Data from Cohu et al. (2013a,b, 2014), Adams et al. (2016,
747 2018a), and Stewart et al. (2016, 2017a,b). Lines of fit with 95% confidence intervals (black
748 lines and gray shading).

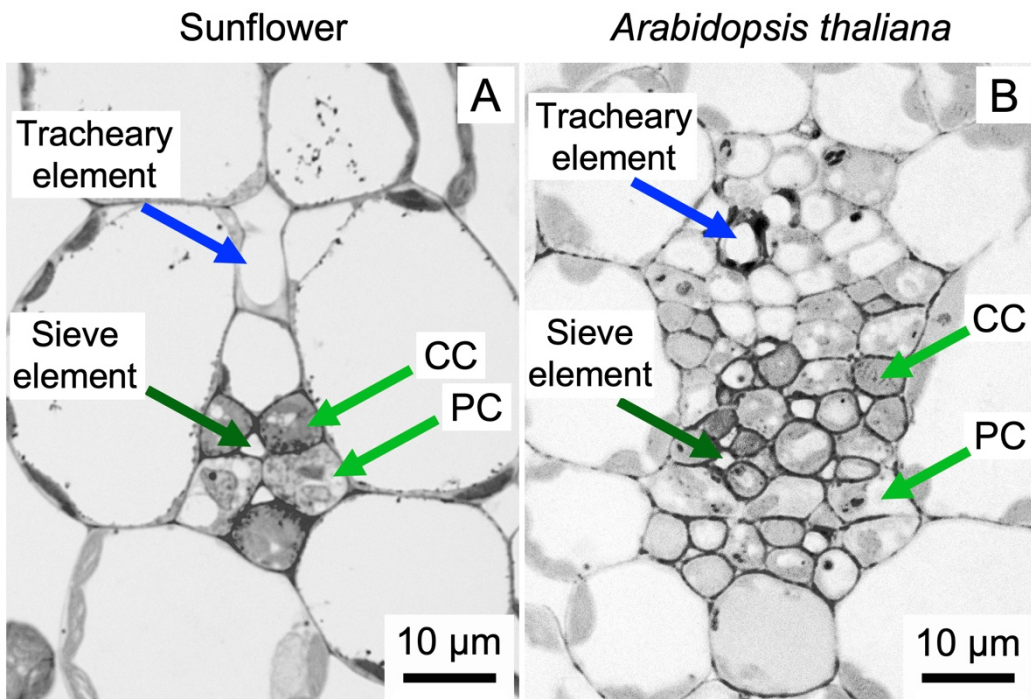
749

750 Fig. 4. Relationship between the cross-sectional areas per minor vein of (A) companion cells +
751 phloem parenchyma cells (CC + PC) and sieve elements and (B) tracheary elements and sieve
752 elements in leaves of *Arabidopsis thaliana* (green symbols), sunflower (*Helianthus annuus*;
753 orange symbols), and spinach (*Spinacia oleracea*; dark green symbols). See the legends of Figs.
754 2 and 3 for additional details. Data from Cohu et al. (2013a,b, 2014), Adams et al. (2016,
755 2018a), Stewart et al. (2017a,b), and Polutchko et al. (2021). Lines of fit with 95% confidence
756 intervals (black lines and gray shading).

757

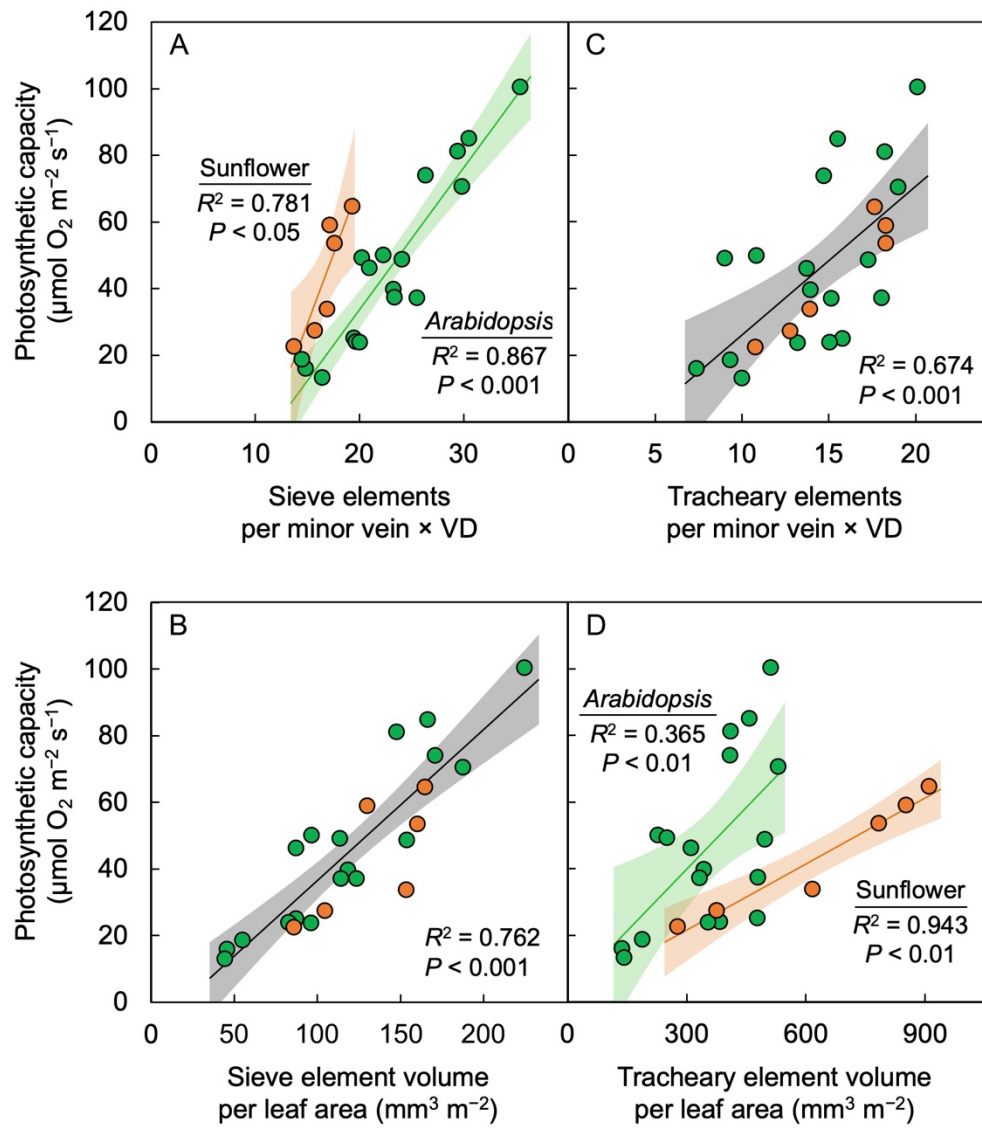
758 Fig. 5. Relationship between the volumes per leaf area of (A) companion cells + phloem
759 parenchyma cells (CC + PC) and sieve elements and (B) tracheary elements and sieve elements
760 in leaves of *Arabidopsis thaliana* (green symbols), sunflower (*Helianthus annuus*; orange
761 symbols), and spinach (*Spinacia oleracea*; dark green symbols). See the legends of Figs. 2 and 3
762 for additional details. Data from Cohu et al. (2013a,b, 2014), Adams et al. (2016, 2018a),
763 Stewart et al. (2017a,b), and Polutchko et al. (2021). Lines of fit with 95% confidence intervals
764 (black lines and gray shading).

765 Fig. 1.



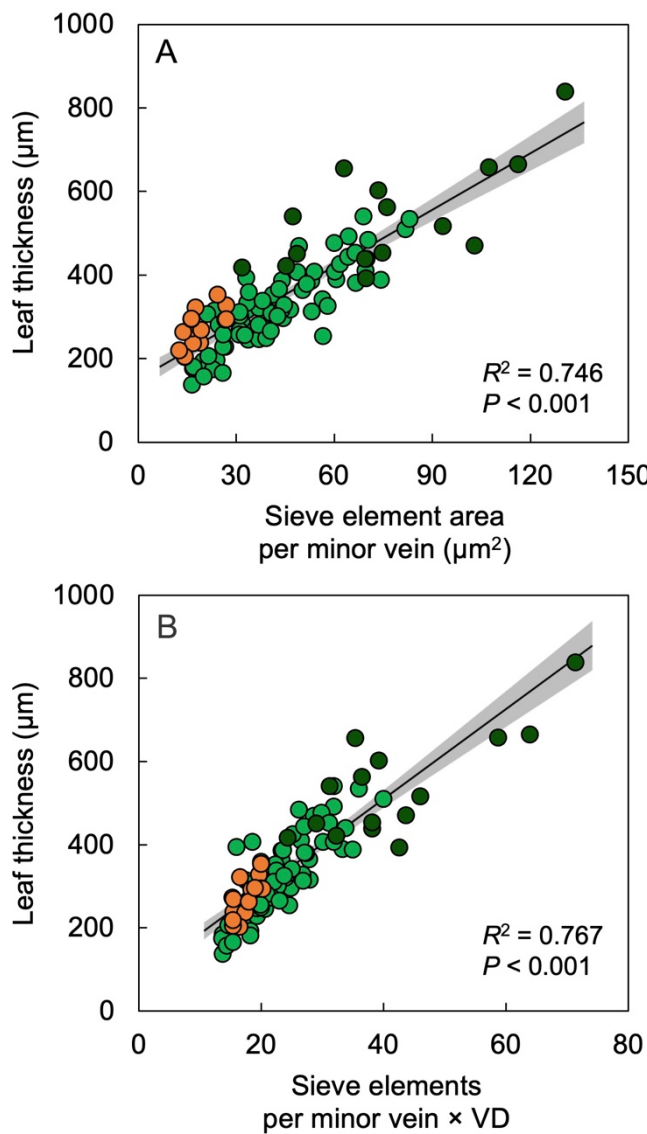
766

767 Fig. 2.



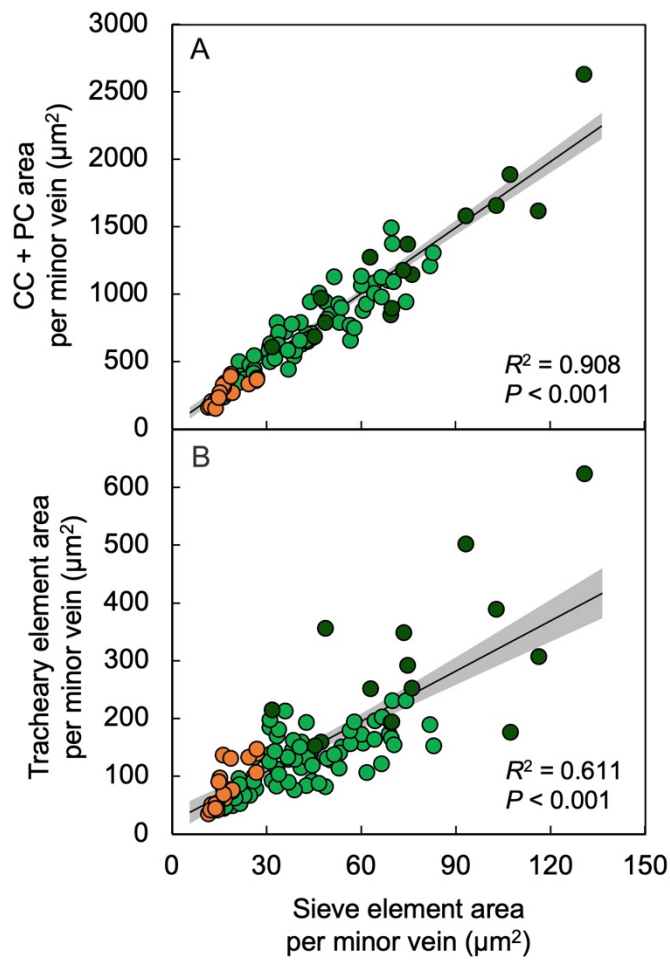
768

769 Fig. 3.



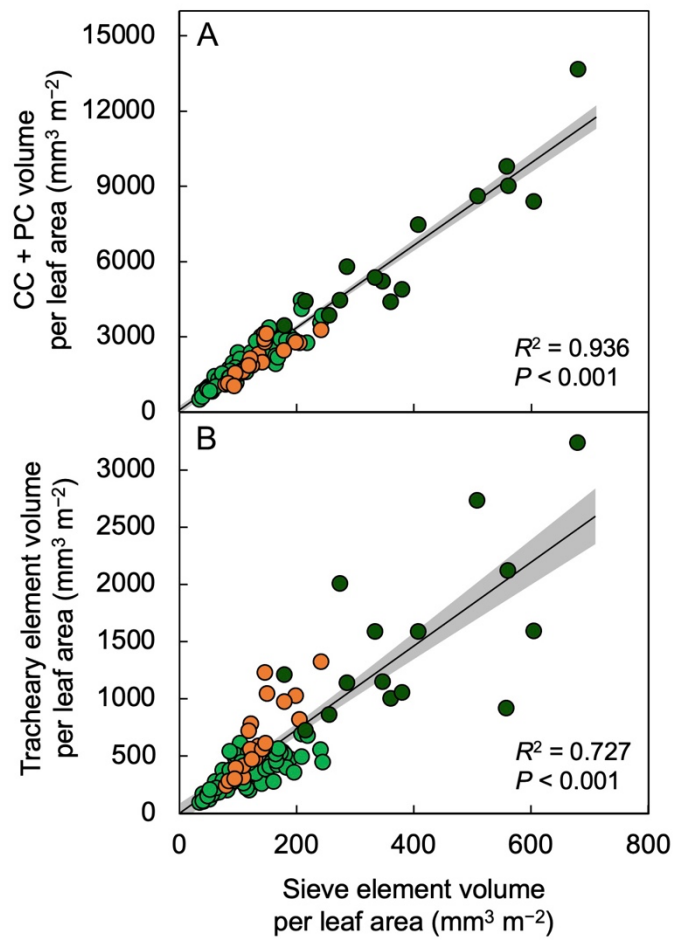
770

771 Fig. 4.



772

773 Fig. 5.



774